



Additive manufacturing of Cu/Ni by selective electrochemical deposition on local conductive substrate

Chenghan Zhao¹ · Jing Wang¹ · Tianyu Liu¹ · Jinyu Guo¹ · Wenzheng Wu¹

Received: 4 November 2022 / Accepted: 10 April 2023 / Published online: 27 April 2023
© The Author(s), under exclusive licence to Springer-Verlag London Ltd., part of Springer Nature 2023

Abstract

Electrodeposition is a novel and benign fabrication method which excellently combines electrochemical deposition mechanism and additive manufacturing to realize the processing of metal-based structures layer-upon-layer. Herein, an unusual additive manufacturing (AM) method is proposed based on electrochemical deposition. Notably, three-dimensional forming of metal by local conductive samples (PLA-CNTs_{7wt%}) as cathode through selective electrochemical deposition was realized. Moreover, the effect of the deposition time on the surface morphology and quality of the sample were explored. Besides, the method of preparing metal parts in array type solves the problem of slow electrochemical additive manufacturing (ECAM) and provides a new approach to achieve mass production for industry. Then, the prepared copper-nickel multilayer metal samples realized the ECAM of multi-metals. Finally, the 4D printing effect of copper-nickel bimetallic samples was preliminarily explored, and the feasibility of preparing energy storage elements by selective electrochemical deposition was further proved.

Keywords Multi-metal · Additive manufacturing · Selective electrochemical deposition · Electrochemical additive manufacturing

1 Introduction

Additive manufacturing (AM) applies specific methods to build materials and uses energy sources to connect processed materials to form 3D parts [1, 2] layer by layer [3], leading to on-demand manufacturing with the least post-processing, smaller operating footprint, and maximum material utilization [4], providing a novel approach to integrate the manufacturing of macro and micro structure parts [5, 6].

Recently, the metal AM has emerged as a significant issue [7, 8], but most mature AM of metal applies high-energy beams as heat to melt metal powder or wire to construct components [9, 10], of which laser is widely used [11], leading to high energy consumption and cost, with residual internal stress. Hence, the electrochemical additive manufacturing (ECAM) stands out which can form 3D entities of any shape, ultimately to realize the directional deposition of metals [12]

with the following advantages: extensive range of the processed material (zinc [13], copper [14], nickel, gold, silver, cobalt [15], alloys [16], conductive polymer [17], etc.), low cost and operating environment requirements, and benign coordination of organization, morphology, and performance.

With the increasing commercial applications of AM, there is an urgent demand for printing multi-materials in a single component [18], leading to an emerging research on multi-material additive manufacturing (MMAM) [19]. Compared with general methods, MMAM brings a higher level of design freedom [20]. The AM of polymetallic materials is mainly based on laser source with defects such as pores, cracks, and delamination at interface.

Whereas processing bimetal parts with ECAM requires no high-temperature heat, without residual thermal stresses and defects [21], depicting an expanse prospect in the development and application of preparing multi-element metal parts.

Herein, a novel AM method associated with electrochemical deposition was adopted. Firstly, local conductive samples were prepared as substrate with polylactic acid (PLA) and carbon nanotube wires (CNTs), further to selectively deposit metal parts, and prepare copper-nickel multi-layer samples, for realizing the ECAM of metals and multi-metals, which proved the feasibility of multi-metal parts processing

Chenghan Zhao and Jing Wang as co-first authors.

✉ Wenzheng Wu
wzwu@jlu.edu.cn

¹ School of Mechanical and Aerospace Engineering, Jilin University, Changchun 130025, Jilin, China

by ECAM. On account of the different thermal expansion coefficients of heterogeneous metals, the 4D printing effect of copper-nickel bimetallic samples was preliminarily explored, as well the viability of preparing energy storage elements by selective electrochemical deposition was demonstrated.

2 Experimental and methods

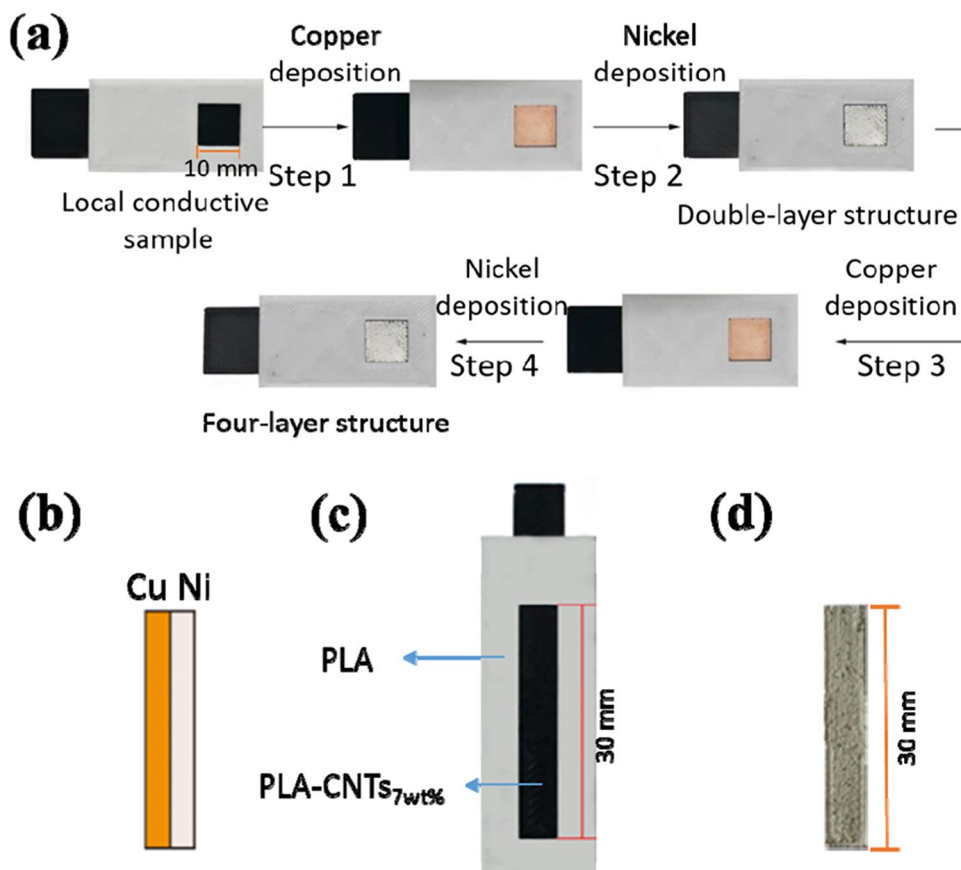
First, the filament preparation was performed with PLA powder (100 mesh, Nature Works, USA) and industrial CNT powder (TN1M1, Chengdu Organic Chemistry Co., Ltd., Chinese Academy of Sciences, China). A dual-nozzle 3D printer (P3, Polar bear, China) was used to prepare local conductive plastic samples. Figure 1c displays the local conductive plastic samples prepared by the dual-nozzle 3D printer, the black area in the part is conductive, composed of polylactic acid-carbon nanotube composite material (PLA-CNTs_{7wt%}). While the white part is insulating, consisting of thermoplastic PLA. Before deposition, the copper plates and local conductive plastic samples were pretreated by rust removal, oil removal, and distilled water cleaning. Later, a local conductive plastic sample was deposited in electrolyte, taking the copper plate as anode and the local conductive

sample as cathode. Then, a sample with metal deposited on the surface of the conductive region was obtained.

The preparation of bimetallic parts is shown in Fig. 1a. Firstly, local conductive plastic sample 1 was deposited with copper in electrolyte A (100 g/L $\text{CuSO}_4 \cdot 5\text{H}_2\text{O}$, 5 vol% H_2SO_4 , and 200 mg/L PEG) (step 1), then electrodeposited with nickel in electrolyte B (100 g/L $\text{NiSO}_4 \cdot 6\text{H}_2\text{O}$ and 25 g/L H_3BO_3) (step 2). After, the sample was removed, cleaned with distilled water, and dried, then the obtained bimetal sample 1 was for standby. Local conductive plastic sample 2 was obtained by repeating step 1 and step 2 for two times to get four-layer metal sample 2 for standby. Besides, the binding of metal interfaces was observed under metal microscope and scanning electron microscope.

As shown in Fig. 1b, the design of bimetal sample is composed of copper and nickel. Figure 1c depicts the local conductive plastic sample. Subsequently, put the sample in electrolyte A for depositing 6 h on 20 mA. After cleaning and drying, the sample was placed in electrolyte B for depositing 6 h on 15 mA. Later, the sample was taken out, cleaned with distilled water, dried, and heated in oven until the plastic softens, and then the metal part was removed from plastic substrate to obtain the bimetallic sheet parts as shown in Fig. 1d. Finally, heated the bimetallic sheet sample with alcohol lamp and observe its deformation.

Fig. 1 **a** Schematic diagram of preparation process of bimetal sample. **b** Model design of bimetal sheet. **c** Local conductive plastic sample. **d** As-deposited bimetal sheet (the nickel side is up)



To demonstrate the electrical properties of electronic components fabricated through selective electrochemical deposition, a 3D spiral coil and interdigitated battery were designed and fabricated.

3 Results and discussion

The prepared plastic sample, as shown in Fig. 2a, was put into the electrolyte A; the spiral coil after electrodeposition is shown in Fig. 2b. Using an impedance analyzer to measure the inductance and impedance of spiral coils. And the magnetic field generated by the solenoid was measured by a gauss meter at different current intensities.

Then prepared a plastic interdigitated battery sample as shown in Fig. 2c. Connect the end of A to anode of the power supply, and the phosphor copper plate to cathode. Subsequently, the sample was electrodeposited in 200 ml electrolyte (20 g $\text{CuSO}_4 \cdot 5\text{H}_2\text{O}$, 10 ml H_2SO_4 , and 40 mg PEG) for 6 h at 30 mA, washed in distilled water to remove residual electrolyte. Afterward, connect the end of B in the sample to the anode of the power and cathode to zinc. Electrodeposited the sample in 200 mL electrolyte (60 g $\text{ZnSO}_4 \cdot 7\text{H}_2\text{O}$, 6 g H_3BO_3) for 6 h at 30 mA. After cleaning, the sample as shown in Fig. 2d was obtained.

After the ends A and B of the sample are connected to the wire and the voltmeter (range 1 V), the sample is placed in 10 vol% sulfuric acid, and the deflection of the voltmeter is observed. When putting the sample into sulfuric acid, the pointer of voltmeter is deflected, and stable at about 0.4 V as shown in Fig. 2e. Zinc on the sample reacts with the sulfuric acid, so the plastic substrate is exposed, the electrons lost by zinc atoms flow to copper through the wire, and zinc atoms are oxidized to zinc ions; meanwhile, hydrogen escapes from the copper surface, hydrogen ions get electrons and reduce to hydrogen, and electrons are transferred from B to A, thus the current is from A to B. The prepared copper-zinc battery can generate a voltage of 0.4 V, demonstrating the outstanding

ability of energy storage elements with excellent electrical communication, and computer technology. The selective electrochemical deposition additive manufacturing is simple in operation, low in cost, and saves complex installations and molds, and has huge advantages in micro-scale electronic components. Local conductive plastic samples after depositing copper in electrolyte (100 g/L $\text{CuSO}_4 \cdot 5\text{H}_2\text{O}$) were shown in Fig. 3a, in which copper was well deposited in the conductive area of square, cross, and strip samples respectively.

Moreover, the deposition is uniform and even micron scale electronic circuits play a crucial role in the network without obvious defects, fully proving the feasibility of selective electrochemical deposition of metal on the local conductive substrate.

As shown in Fig. 3b, the copper sheets all hold intact square shape and uniform deposition overall. Afterwards, the micro morphology of the upper surface on metal sheet was observed by scanning electron microscope (SEM, JSM-IT500A, JEOL, Japan) as shown in Fig. 4a–e. With the gradual increase of deposition time from 2, 4, 6, 8 to 10 h, the grain size of copper rises, corresponding to the aggravated surface roughness. Among them, the metal sheet for 2 h shows the smoothest surface morphology without uneven bulge and particle defects and exhibits uniform grain size in the SEM image of its upper surface.

According to Fig. 3c, with the deposition time lengthening, the mass of the samples gradually rises in linear relation, indicating the current efficiency remains in a relatively stable state during the increasing deposition time. It demonstrates, as the deposition time increases, preparing the metal parts by the selective electrochemical deposition can achieve the relatively stable current efficiency and obtain the roughly steady quality of the metal per unit.

The complex 3D metal components, helical line, and hollow sphere prepared are shown in Fig. 5a and b. The resulting black material on the surface of the 3D metal parts corresponds to carbonized PLA and residual CNTs.

Fig. 2 **a** Plastic spiral coil prepared by 3D printer. **b** As-deposited Cu spiral coil. **c** Plastic interdigitated battery prepared by 3D printer. **d** Interdigitated battery after electrodeposition of copper and zinc. **e** Discharge process of interdigitated battery

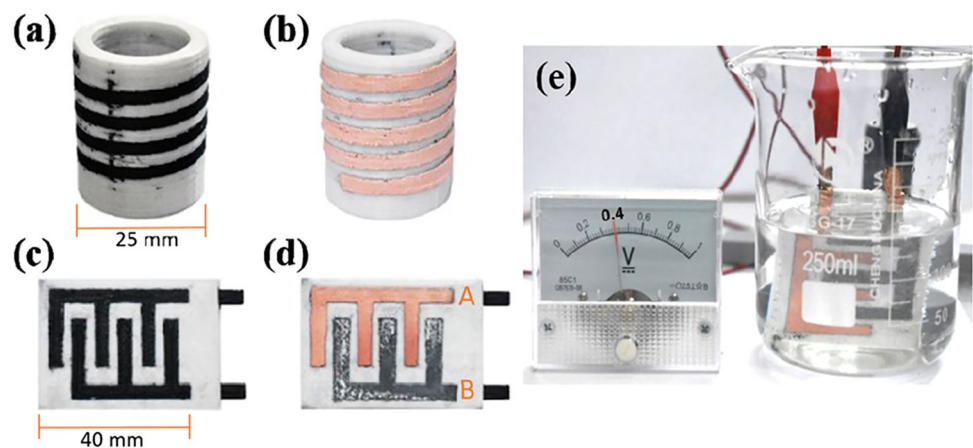
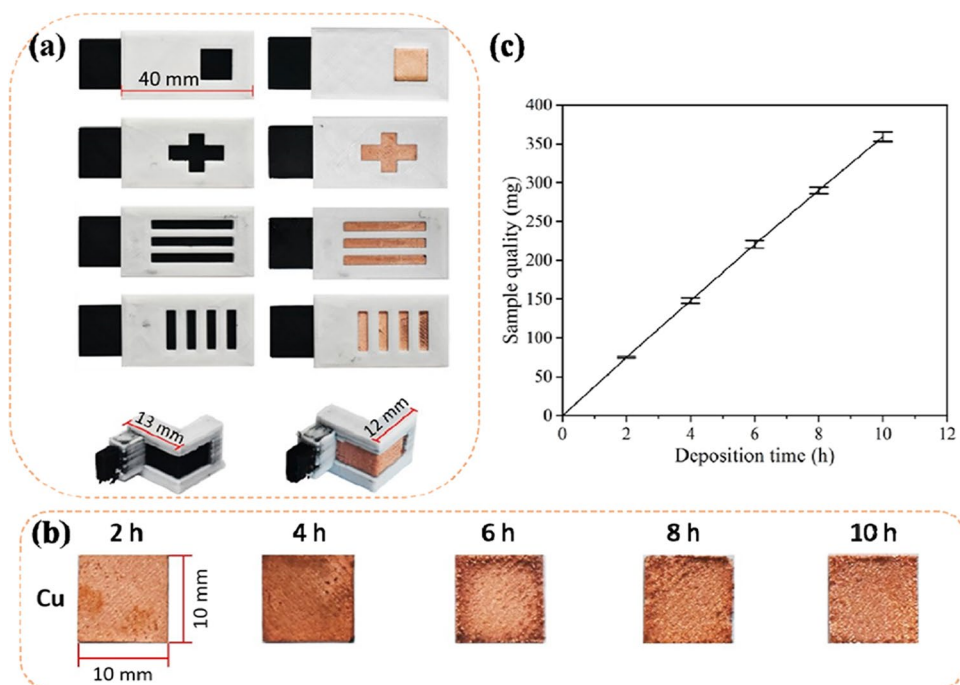


Fig. 3 **a** Variform local conductive plastic samples and selective electrochemical deposition samples. **b** The photograph of metal samples under different deposition time. **c** Diagram of sample quality variation over deposition time



When heating the bimetal sheet sample by an alcohol lamp, with the extended time, the sample gradually bent to the side of nickel, and the deflection angle increased likewise. When returning to room temperature, the sample generally returned to the original shape, as shown in Fig. 5c.

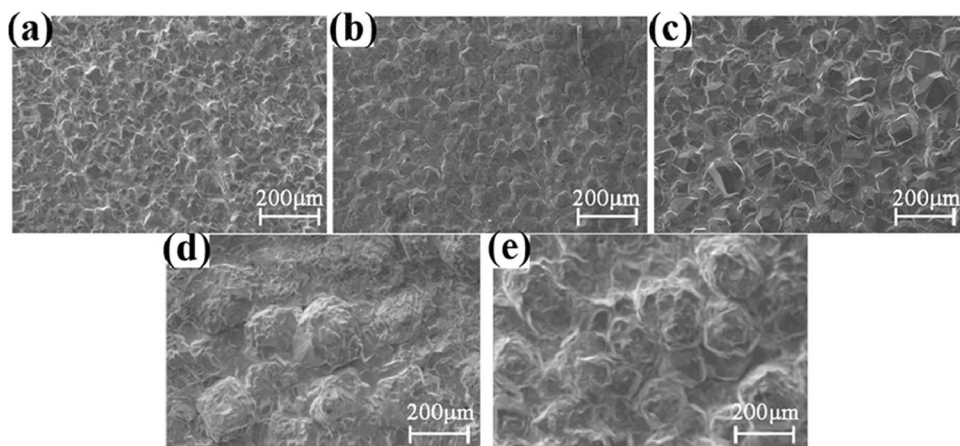
Owing to the greater linear expansion coefficient of copper than nickel, when heated equally, the thermal deformation length of copper is greater than nickel; hence, the sample will deflect to the side of the nickel. When returned to room temperature, the thermal expansion part of copper and nickel will shrink, namely, the sample will roughly return to its original shape.

When a layer of copper with identical thickness is deposited on the other side of nickel, the thermal deformation of copper on both sides will cancel when heated, and the sample will not be bent in this area, so the sample can be

programmed and designed. According to the design intent, the specific area of the sample can be processed into a three-layer structure of copper-nickel-copper or nickel-copper-nickel, while the other parts have a double-layer structure of copper-nickel, as shown in Fig. 5d. During heating the sample, a specific area will bend, while other areas will remain in their original state. It is also possible to adjust the distribution direction of copper and nickel in each double-layer metal area to regulate the bending direction of the sample.

As shown in Fig. 5e–h, there appeared defects in the four deposition areas of sample e that no metal was deposited at 30 mA, indicating too less copper was produced to fully cover the deposition areas. Whereas the deposition in two areas on the left of sample f was uniform without defects at 40 mA, there existed more obvious defects in two areas on the right. Further increasing the current to 50 mA, there

Fig. 4 The influence of different deposition time on surface morphology of upper surface of samples (a 2 h, b 4 h, c 6 h, d 8 h, e 10 h at same current 20 mA)



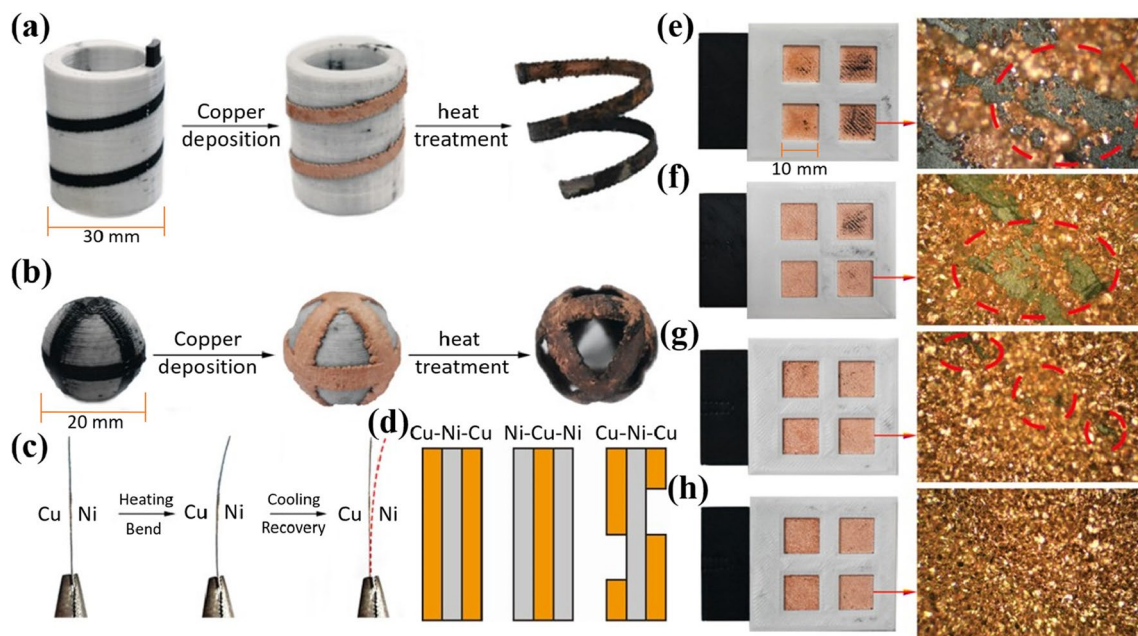


Fig. 5 **a** Preparation procedure of helical line. **b** Preparation procedure of hollow sphere. **c** 4D deformation process of bimetallic samples. **d** Schematic diagram of programmable samples. **e** The array-

type ECAM samples under different deposition current (**e** 30 mA, **f** 40 mA, **g** 50 mA, **h** 60 mA)

showed only a few defects in the upper right area of the sample **g**, demonstrating the further increased quality of deposition. When tuning to 60 mA, no defects occurred in sample **h**, exhibiting the highest deposition quality and complete coverage in the equal deposition areas. In addition, the grain size of deposited copper remains uniform roughly under the four current intensities, illustrating the increased current intensity did not obviously change the morphology of the metal layer, and can also enhance the deposition quality through elevating current intensity. Therefore, if the array structure sample has enough deposition area and appropriate current intensity, it can simply realize the large-scale production of metal electrochemical additive manufacturing.

The edge section of bimetal sheet 1 and four-layer metal sheet 2 was ground with sandpaper, then observed the cross-sectional morphology by metallurgical microscope. Through Fig. 6a and c, the copper layer and nickel layer were well combined with no gaps between layers. Subsequently, cut the sheet 1 and sheet 2 in the middle, and observe the cross-section of the middle part of the sheets. In view of Fig. 6b and d, the thickness of the middle is slightly smaller than the edge; the copper layer and nickel layer combine tightly in the middle with no cracks.

The fracture morphology of sheets 1 and 2 is legible to observe, and the thickness of each layer was roughly measured. Figure 6e shows the upper metal of sheet 1 is nickel with a thickness of about 112.0 μm and the lower metal is copper with a thickness of about 98.54 μm . In addition, the morphology of the fracture surface of sheet 2 is shown in

Fig. 6f, wherein layers are nickel, copper, nickel, and copper from top to bottom, and the thickness is 79.91, 88.09, 50.78, and 76.67 μm separately. In addition, the bimetallic strip has a compact metal structure and its layers are closely bonded, which fully proves the superiority of this method in preparing multi-metal parts.

4 Conclusions

In this paper, we applied CNTs as conductive particles to fill the PLA matrix to prepare composite filaments and adopted the fused deposition 3D printer with dual nozzle to obtain local conductive samples. Later, the samples were deposited layer by layer through selective electrochemical deposition to realize the 3D forming of metal and multi-metal, and a method for separating the formed metal from the plastic substrate was proposed. Additionally, the effect of deposition time on the surface morphology and quality of the sample was explored. With the extension of deposition time, the grain size on the surface and the quality of the sample increases, as well the rate of deposition shows relatively stable wholly. In addition, the concept of preparing metal parts in an array and amplifying current density improves the deposition quality and coverage area. It accelerates the speed of processing and exhibits a handy approach for additive manufacturing to achieve mass production. At the same time, the prepared multi-metal parts are closely combined between different metal layers and 4D printing performance of the parts was studied. In consequence, the 4D printing function

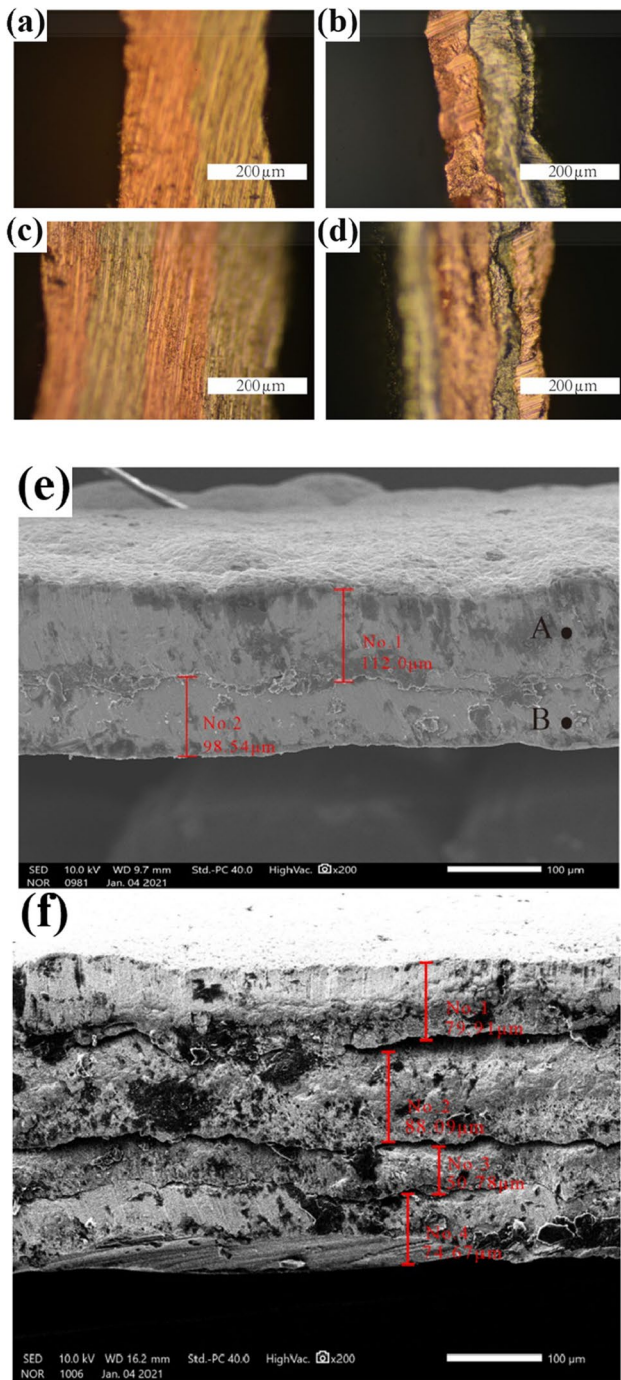


Fig. 6 Metallurgical microscope image of samples. **a** Cross-section morphology of bimetal sample. **b** Fracture morphology of bimetal sample. **c** Cross-section morphology of four-layer metal sample. **d** Fracture morphology of four-layer metal sample. **e** SEM image for the fracture surface of bimetal sheet 1. **f** SEM image for the fracture surface of four-layer metal sheet 2

can be applied to relays, switches, controllers, etc. In conclusion, designing the two metal arrangement positions in the sample and adjusting the distribution direction of each bimetal area, thereby adjusting the bending direction, provides the possibility

to create a more intelligent structure and sensor. The prepared copper-zinc battery can generate a voltage of 0.4 V, providing a basis for novel fabrication in the field of microelectronics.

Author contribution Chenghan Zhao and Jing Wang played guiding roles in this paper and contributed equally to the article as co-first authors. Wenzheng Wu contributed to the conceptualization, methodology, and resources. Tianyu Liu and Jinyu Guo contributed to experimental investigation and prepared the original draft. Chenghan Zhao and Jing Wang contributed to the data curation, validation, reviewing and editing. All authors have read and agreed to the published version of the manuscript.

Funding This research was supported by National Natural Science Foundation of China (No.52075219) and National Key R&D Program of China (No. 2022YFB4600202).

Data availability Not applicable.

Code availability Not applicable.

Declarations

Ethics approval Not applicable.

Consent to participate Not applicable.

Consent for publication Not applicable.

Competing interests The authors declare no competing interests.

References

- Gao W, Pumera M (2021) 3D printed nanocar-bon frameworks for Li-ion battery cathodes. *Adv Funct Mater* 31(11):2007285. <https://doi.org/10.1002/adfm.202007285>
- Horn T J, Harrysson O L (2012) Overview of current additive manufacturing technologies and selected applications. *Science Progress*, 95(3): 255–282. <https://doi.org/10.3184/003685012X13420984463047>
- Behroozfar A, Daryadel S, Morsali SR, Mor-eno S, Baniasadi M, Bernal RA, Minary-Jolanda-n M (2018) Microscale 3D printing of nanotwin-ned copper. *Adv Mater* 30(4):1705107. <https://doi.org/10.1002/adma.201705107>
- Tofail SAM, Koumoulos EP, Bandyopadhyay A, Bose OS, L, Charitidis C, (2018) Additive manufacturing: scientific and technological challenges, market uptake and opportunities. *Mater Today* 21(1):22–37. <https://doi.org/10.1016/j.mattod.2017.07.001>
- Yao B, Chandrasekaran S, Zhang H, Ma A, Kang J, Zhang L, Lu X, Qian F, Zhu C, Duoss EB, Spadaccini CM, Worsley MA, Li Y (2020) 3D-printed structure boosts the kinetics and intrinsic capacitance of pseudocapacitive graphene aerogels. *Adv Mater* 32(8):e1906652. <https://doi.org/10.1002/adma.201906652>
- Kuang X, Chen K, Dunn CK, Wu J, Li VCF, Qi HJ (2018) 3D printing of highly stretchable, shape-memory, and self-healing elastomer toward novel 4D printing. *ACS Appl Mater Interfaces* 10(8):7381–7388. <https://doi.org/10.1021/acsami.7b18265>
- Seol SK, Kim D, Lee S, Kim JH, Chang WS, Kim JT (2015) Electrodeposition-based 3D printing of metallic microarchitectures with controlled internal structures. *Small* 11(32):3896–3902. <https://doi.org/10.1002/sml.201500177>

8. Gomes MC, dos Santos AG, de Oliveira D, Figueiredo GV, Ribeiro KSB, De Los RGAB, da Silva MB, Coelho RT, Hung WNP (2021) Micro-machining of additively manufactured metals: a review. *Int J Adv Manuf Technol* 118(7–8):2059–2078. <https://doi.org/10.1007/s00170-021-08112-0>
9. Hirt L, Ihle S, Pan Z, Dorwling-Carter L, Reiser A, Wheeler JM, Spolenak R, Vörös J, Zambelli Alain Reiser T (2016) Template-free 3D microprinting of metals using a force-controlled nanopipette for layer-by-layer electrodeposition. *Adv Mater* 28(12):2311–2315. <https://doi.org/10.1002/adma.201504967>
10. Schaffer TB, Sercombe GB (2003) Rapid manufacturing of aluminum components. *Science* 301(5637):1225–1227. <https://doi.org/10.1126/science.1086989>
11. Collins PC, Brice DA, Samimi P, Ghamarian I, Fraser HL (2016) Microstructural control of additively manufactured metallic materials. *Annu Rev Mater Res* 46(1):63–91. <https://doi.org/10.1146/annurev-matsci-070115-031816>
12. Kamaraj AB, Sundaram M (2019) A mathematical model of the deposition rate and layer height during electrochemical additive manufacturing. *Int J Adv Manuf Technol* 102(5–8):2367–2374. <https://doi.org/10.1007/s00170-019-03292-2>
13. Nydegger M, Pruska A, Galinski H, Zenobi R, Reiser A, Spolenak R (2022) Additive manufacturing of Zn with submicron resolution and its conversion into Zn/ZnO core-shell structures. *Nanoscale* 14(46):17418–17427. <https://doi.org/10.1039/d2nr04549d>
14. Hengsteler J, Mandal B, Van Nisselroy C, Lau GPS, Schlotter T, Zambelli T, Momotenko D (2021) Bringing electrochemical three-dimensional printing to the nanoscale. *Nano Lett* 21(21):9093–9101. <https://doi.org/10.1021/acs.nanolett.1c02847>
15. Rolandi M, Okawa D, Backer SA, Zettl A, Fréchet MJM (2007) Fabrication of magnetic force microscopy probes via localized electrochemical deposition of cobalt. *J Vacuum Sci Technol B: Microelectron Nanometer Struct* 25(5):L39–L42. <https://doi.org/10.1116/1.2766935>
16. Pellicer E, Pané S, Panagiotopoulou VC, Fusco S, Sivaraman KM, Suriñach S, Baró MD, Nelson BJ, Sort J & Física D (2012) Localized electrochemical deposition of porous Cu-Ni microcolumns: insights into the growth mechanisms and the mechanical performance. *Int J Electrochem Sci* 7(5):4014–4029. <https://doi.org/10.3103/S1068375512030143>
17. Aydemir N, Parcell J, Laslau C, Nieuwoudt M, Williams DE, Travas-Sejdic J (2013) Direct writing of conducting polymers. *Macromol Rapid Commun* 34(16):1296–1300. <https://doi.org/10.1002/marc.201300386>
18. Roach DJ, Hamel CM, Dunn CK, Johnson MV, Kuang X, Qi HJ (2019) The m⁴ 3D printer: a multi-material multi-method additive manufacturing platform for future 3D printed structures. *Addit Manuf* 29:100819. <https://doi.org/10.1016/j.addma.2019.100819>
19. Kuang X, Qi HJ (2020) Modular 4D printing assisted by dynamic chemical bonds. *Matter* 2(5):1080–1082. <https://doi.org/10.1016/j.matt.2020.04.014>
20. Vaezi M, Chianrabutra S, Mellor B, Yang S (2013) Multiple material additive manufacturing-Part 1: a review. *Virtual Phys Prototyp* 8(1):19–50. <https://doi.org/10.1080/17452759.2013.778175>
21. Xu J, Ren W, Lian Z, Yu P, Yu H (2020) A review: development of the maskless localized electrochemical deposition technology. *Int J Adv Manuf Technol* 110(7–8):1731–1757. <https://doi.org/10.1007/s00170-020-05799-5>

Publisher's note Springer Nature remains neutral with regard to jurisdictional claims in published maps and institutional affiliations.

Springer Nature or its licensor (e.g. a society or other partner) holds exclusive rights to this article under a publishing agreement with the author(s) or other rightsholder(s); author self-archiving of the accepted manuscript version of this article is solely governed by the terms of such publishing agreement and applicable law.